Quantum Metric and Correlated States in Two-dimensional Systems

Enrico Rossi[1, *]

[1]*Department of Physics, William & Mary, Williamsburg, Virginia (23187), USA*

The recent realization of twisted, two-dimensional, bilayers exhibiting strongly correlated states has created a platform in which the relation between the properties of the electronic bands and the nature of the correlated states can be studied in unprecedented ways. The reason is that these systems allow extraordinary control of the electronic bands' properties, for example by varying the relative twist angle between the layers forming the system. In particular, in twisted bilayers the low energy bands can be tuned to be very flat and with a nontrivial quantum metric. This allows the quantitative and experimental exploration of the relation between the metric of Bloch quantum states and the properties of correlated states. In this work we first review the general connection between quantum metric and the properties of correlated states that break a continuous symmetry. We then discuss the specific case when the correlated state is a superfluid and show how the quantum metric is related to the superfluid stiffness. To exemplify such relation we show results for the case of superconductivity in magic angle twisted bilayer graphene. We conclude by discussing possible research directions to further elucidate the connection between quantum metric and correlated states' properties.

I. INTRODUCTION

One of the most exciting developments of the past few years in condensed matter physics has been the ability of experimentalists to realize two-dimensional (2D) "twisted bilayers" [1] and observe the establishment in these systems of strongly correlated electronic states [2–16]. These systems are formed by two 2D crystals stacked with a relative twist angle θ. Twisted bilayer graphene (TBLG), formed by two graphene layers, so far, has been the most studied twisted bilayer system. The feat that experimentalists have been able to accomplish is to control θ with high precision and tune it to particular, "magic", values (θ_M) for which the bands of the system are almost completely flat [17–19]. It is for this magic values of θ that the system exhibits a very rich phase diagram with strongly correlated phases, including a superconducting phase for which the ratio between the critical temperature, T_c, and the Fermi temperature, T_F, ranges between 0.04 and 0.1, depending on the doping [3]. The value of $T_c/T_F \approx 0.1$ is much larger than the one for conventional BCS superconductors, and implies that to understand the origin of superconductivity in MATBLG weak coupling theory is not sufficient. Such value is also larger than in most unconventional superconductors [3], in particular high T_c cuprates.

One very interesting aspect of magic angle twisted bilayer graphene (MATBLG) is the non-trivial geometry of its quantum states. As a consequence MATBLG is a new, highly tunable, platform in which the connection between strong correlations and quantum states' geometry can be explored in detail both theoretically and experimentally. This allows to significantly advance our understanding of the relation between the metric of quantum states, the conditions necessary for the establishment and stability of strongly correlated states, and the properties of these states.

For the past fifteen years the geometry of quantum states has been at the center of some of the most interesting discoveries in condensed matter physics. The geometry of a manifold of quantum states is encoded by the "quantum geometric tensor", $Q_{\mu\nu}$ [20–23]. $Q_{\mu\nu}$ has both a real and an imaginary part. The imaginary part of $Q_{\mu\nu}$ corresponds to the Berry curvature [24]. In the past few years many interesting developments in condensed matter physics have arisen by a careful treatment of the Berry curvature. Exemplary are the the discovery of topological insulators (TIs) and superconductors [25–29], Weyl and Dirac semimetals (SMs) [30–33], and, more recently, higher order topological materials [34–42]. At the same time, it is interesting to notice how much less attention the real part of $Q_{\mu\nu}$, $\mathrm{Re}[Q_{\mu\nu}]$, the "quantum metric", has received compared to its imaginary part. This is in great part due to the difficulty to measure physical quantities related to $\mathrm{Re}[Q_{\mu\nu}]$. However, the connection between quantum metric and the properties of collective ground states breaking a continuous symmetry, and the availability of a system like MATBLG, have opened a new avenue to understand how $\mathrm{Re}[Q_{\mu\nu}]$ can affect the macroscopic properties of quantum systems.

In this work we briefly review the recent progress in the understanding of the relation between quantum metric and the properties of correlated states of 2D systems. In section II we present the formalism describing in general terms the relation between quantum metric and correlated states, in section III we discuss the case when the correlated state is a superconductor, in section IV we review some of the recent results for MATBLG, and finally in section V we summarize the current status of our understanding of the topic and possible developments in the near future.

II. QUANTUM METRIC AND PROPERTIES OF MANY-BODY SYSTEMS

Quantum mechanical states are represented by rays in a complex Hilbert space. For a given quantum system, therefore, the space of physical states is not the Hilbert space $\mathcal{H}$, but the projective Hilbert space $\mathcal{P}_\mathcal{H}$. The projective Hilbert space $\mathcal{P}_\mathcal{H}$ is the space formed by rays in the Hilbert space $\mathcal{H}$, where each ray is the set of vectors in $\mathcal{H}$ of unit norm that differ only by multiplication by phase factors. For a Hilbert space of dimension n, $\mathcal{P}_\mathcal{H}$ is the complex projective space

* Corresponding author: erossi@wm.edu

$\mathbb{C}P^{n-1}$ formed by the lines through the origin of a complex Euclidean space. The inner-product of $\mathcal{H}$ endows $\mathcal{P}_{\mathcal{H}}$ with the structure of a Kähler manifold, i.e. a manifold with a a proper metric tensor [43; 44]. $\mathcal{P}_{\mathcal{H}}$ can be parametrized by an element λ of a space $\mathcal{V}$ (that itself can be a manifold) like real space, or momentum space. In the remainder we assume the space $\mathcal{V}$ to be the momentum space with elements identified by the momentum wave-vector $\mathbf{k}$.

The inner product of $\mathcal{H}$ leads to the natural definition of the distance ds^2 between two vectors $|\psi(\mathbf{k})\rangle$, $|\psi(\mathbf{k}+d\mathbf{k})\rangle$ with infinitesimally close momenta, $\mathbf{k}$, $\mathbf{k}+d\mathbf{k}$: $ds^2 = \langle\partial_\mu\psi|\partial_\nu\psi\rangle dk^\mu dk^\nu$, where $\partial_\mu \equiv \partial/\partial k_\mu$. Given that quantum states are represented by elements of $\mathcal{P}_{\mathcal{H}}$, not $\mathcal{H}$, the expression of ds^2 is not the proper distance between two quantum states with infinitesimally close momenta. This is also reflected by the fact that $\langle\partial_\mu\psi|\partial_\nu\psi\rangle$, in general, is not gauge invariant. The proper distance between quantum states can be obtained by redefining ds^2 to remove the effects of a gauge transformation [20–23]. This leads to the expression:

$$ds^2 = Q_{\mu\nu} dk^\mu dk^\nu; \tag{1}$$

$$Q_{\mu\nu} \equiv \langle\partial_\mu\psi|\partial_\nu\psi\rangle - \langle\partial_\mu\psi|\psi\rangle\langle\psi|\partial_\nu\psi\rangle \tag{2}$$

$$B_{\mu\nu} \equiv \text{Im}[Q_{\mu\nu}] \tag{3}$$

$$g_{\mu\nu} \equiv \text{Re}[Q_{\mu\nu}] \tag{4}$$

where we have introduced the *quantum geometric tensor* $Q_{\mu\nu}$. $Q_{\mu\nu}$ is gauge invariant. Its imaginary part is the Berry curvature, $B_{\mu\nu}$, and is completely antisymmetric and therefore does not contribute to ds^2. Its real part, $g_{\mu\nu}$, is the Fubini-Study quantum metric [45; 46]. It is interesting to point out that the Fubini-Study metric is the unique Riemannian metric on $\mathcal{P}_{\mathcal{H}}$ that is invariant under the action of unitary transformations ($U(n)$) on CP^{n-1}. The quantum geometric tensor $Q_{\mu\nu}$ is positive semidefinite [20]. This fact implies the following two inequalities [47]:

$$\det g_{\mu\nu} \geq |B_{\mu\nu}|^2, \tag{5}$$

$$\text{Tr}g_{\mu\nu} \geq 2|B_{\mu\nu}| \tag{6}$$

It is possible to generalize the definition of $Q_{\mu\nu}$ to the non-Abelian case [48], in analogy to the non-Abelian generalization of the Berry curvature [49]. In this generalization one takes into account that at the degeneracy points quantum states related by a rotation in the subspace spanned by the degenerate eigenstates are equivalent. By properly projecting $\langle\partial_\mu\psi|\partial_\nu\psi\rangle$ one obtains the gauge invariant "non-Abelian" quantum metric.

The impact of the study of the effects of the Berry curvature $\text{Im}[Q_{\mu\nu}]$ on the properties of quantum systems cannot be overstated. Just in the context of condensed matter systems the Berry curvature, and associated Berry phase [24], greatly impacted the understanding of the quantum Hall effect, the anomalous Hall effect, orbital magnetism [50] and it lead to the discovery of topological materials [27; 51], and Weyl semimetals [32]. By contrast the effect of $\text{Re}[Q_{\mu\nu}]$ has so far been much less studied. $g_{\mu\nu}$ has been shown to be connected to the Hall viscosity [52–60], a quantity that is difficult to measure [61–67]. For a perfect conductor the longitudinal electric conductivity $\sigma_{xx}(\omega)$ as a function of frequency ω

has a delta function $D\delta(\omega)$, where D is the Drude weight. The Drude weight has also been shown to be connected to the quantum metric $g_{\mu\nu}$, [68–71]. Such connection, however, is also difficult to ascertain experimentally given that at finite temperature, or in the presence of any amount of disorder, $\sigma_{xx}(\omega)$ does not have a Dirac's delta for $\omega = 0$ and therefore $D = 0$.

The experimental challenges to verify the relation between $g_{\mu\nu}$, the Hall viscosity, and D are likely an important reason for the fact that much less research activity has been focused on the study of the effects of the quantum metric than on the study of the effects of the Berry curvature. Recently, however, novel connections [47; 72–78] have been made between the quantum metric and properties of electronic systems. In Refs. [47; 72] the quantum metric of a fractional Chern insulator [79] has been bee shown to be related to the stability of the fractional quantum Hall (FQH) phase of these systems. In particular it was shown that for a fractional Chern insulator band j the trace $\text{Tr}[g_{\mu\nu}^{(j)} - |B_{\mu\nu}|]$ is correlated to the gap of the FQH-like phase [72]. It is also known that the magnetic susceptibility of a periodic multi orbital electron system depends on the metric properties of the quantum states [73; 74; 80]. In Ref. [75] this connection has been made more explicit for the case of two-band models. The metric tensor of a singular 2D flat band [81], i.e. a flat band with a crossing point with a dispersive band, has also been shown to be connected to the *energy spread* of the Landau levels arising from the singular 2D flat band in the presence of a magnetic field [76].

For systems in which the interactions induce a collective ground state that breaks a $U(1)$ symmetry it has become apparent that the quantum metric is connected to the phase *stiffness*, $\rho_{\mu\nu}^{(s)}$, of the collective ground state. This can be seen considering that in this case the effective Ginzburg-Landau action describing the low energy physics of the collective ground state has a term of the form

$$S = \beta\frac{1}{2}\int d\mathbf{r}\rho^{(s)}|\nabla\psi|^2 \tag{7}$$

where $\psi = \psi_0 e^{i\phi}$ is the complex order parameter describing the ground state, ψ_0 being the amplitude and ϕ the phase parametrizing $U(1)$, and $\beta = 1/(k_B T)$, T being the temperature and k_B the Boltzmann constant. To simplify the notation in Eq. (7) we have assumed the stiffness to be diagonal and isotropic $\rho_{\mu\nu}^{(s)} = \rho^{(s)}\delta_{\mu\nu}$. We can then introduce a gauge field $\mathbf{A}_{\text{eff}}$ associated to the $U(1)$ charge $\tilde{e}$. In the presence of $\mathbf{A}_{\text{eff}}$ the gradient in Eq. (7) must be replaced by the gauge covariant gradient $\nabla - i\tilde{e}\mathbf{A}_{\text{eff}}$ from which we get mix terms of the form $-i\tilde{e}\mathbf{A}_{\text{eff}}\nabla$ that describe the coupling of the system to the field $\mathbf{A}_{\text{eff}}$. From this we can see that that the current operator $\mathbf{j}$ coupling to $\mathbf{A}_{\text{eff}}$ is $\sim \tilde{e}\nabla_{\mathbf{x}}$, and that ρ_s must be related to the strength of the current-current response (K) of the system to the probing field $\mathbf{A}_{\text{eff}}$. This is completely analogous to the case of a superconductor, discussed in the next section, in which the connection between the metric of the quantum states and $\rho_{\mu\nu}^{(s)}$ is shown explicitly. This connection was first shown explicitly for simple cases in superconductors [82–84] and for flat ferromagnetic states in systems with flat bands [85].

Among all the types of condensed matter systems in which the ground states spontaneously break a $U(1)$ symmetry two are particularly important and common: ferromagnets (FMs) and superconductors (SCs). For both classes of systems $\text{Re}[Q_{\mu\nu}]$ can play an essential role in determining the properties of the collective ground state. For magnetic systems $\text{Re}[Q_{\mu\nu}]$ enters the expression of the spin-stiffness, $\rho_{\mu\nu}^{(\text{s,spin})}$, for superconductors it contributes to the superfluid stiffness, $\rho_{\mu\nu}^{(\text{s})}$, or, equivalently, the superfluid weight $D_{\mu\nu}^{(\text{s})}$. $\rho_{\mu\nu}^{(\text{s,spin})}$ and $\rho_{\mu\nu}^{(\text{s})}$ can be measured and are not affected by small amounts of disorder and so their relationship to $\text{Re}[Q_{\mu\nu}]$ can be verified experimentally.

For 2D systems for which the ground state spontaneously breaks a U(1) symmetry, $\rho_{\mu\nu}^{(\text{s})}$ governs the Berezinskii-Kosterlitz-Thouless [86; 87] (BKT) transition, in particular it fixes the value of the temperature, T_{KT}, at which the transition takes place. For an isotropic system $\rho_{\mu\nu}^{(\text{s})} = \rho^{(\text{s})}\delta_{\mu\nu}$ and $\rho^{(\text{s})}$ fixes T_{KT} via the relation [87]:

$$k_B T_{KT} = \frac{\pi}{2}\rho^{(s)}(T_{KT}). \qquad (8)$$

As we discuss in the following two sections, equation (8) can be used to estimate the value of ρ_s in 2D systems.

For a multi-orbital system $\rho_{\mu\nu}^{(\text{s})}$ has a contribution due to the curvature of the bands, the so called "conventional" contribution, $\rho_{\mu\nu}^{(\text{s,conv})}$, and a contribution due to $\text{Re}[Q_{\mu\nu}]$, the so called "geometric" contribution, $\rho_{\mu\nu}^{(\text{s,geo})}$. $\text{Re}[Q_{\mu\nu}]$ can be different from zero only for multiband systems. It is therefore clear that the geometric contribution to $\rho_{\mu\nu}^{(\text{s})}$ can be dominant in multi-orbital systems with flat bands. This is precisely the situation in MATBLG: the effective moiré lattice of MATBG has a multiband spectrum with the lowest energy bands, the ones that participate in the formation of collective ground states such as superconducting and ferromagnetic states [88–90], extremely flat. The advent of systems like MATBLG has then greatly increased our ability to study and understand the relation between the metric of quantum states and the macroscopic properties of collective ground states.

III. QUANTUM METRIC AND SUPERFLUID STIFFNESS

To exemplify in concrete terms the connection between the quantum metric and the stiffness of a ground state breaking a $U(1)$ symmetry we consider the case of a superconductor. For the linear current response to an external vector potential, in momentum and frequency space we have

$$j_\mu(\mathbf{k},\omega) = K_{\mu\nu}(\mathbf{k},\omega)A_\nu(\mathbf{k},\omega) \qquad (9)$$

where $j_\mu(\mathbf{k},\omega)$, $A_\mu(\mathbf{k},\omega)$, and $K_{\mu\nu}(\mathbf{k},\omega)$ are the Fourier amplitude with wave vector $\mathbf{k}$ and frequency ω of the μ component of the current density, the μ component of the vector potential $\mathbf{A}$, and of the $\mu\nu$ component of the current-current response function, respectively. The superfluid weight, $D_{\mu\nu}^{(\text{s})}$ is the tensor that relates, within the linear approximation, j_μ

to the ν component of a static ($\omega = 0$) transverse vector potential, $\mathbf{k} \cdot \mathbf{A} = 0$, in the limit $\mathbf{k} \to 0$. Denoting by $k_\parallel$, $k_\perp$, the components of $\mathbf{k}$ parallel and perpendicular to $\mathbf{A}$, respectively, we have [91; 92]:

$$D_{\mu\nu}^{(\text{s})} \equiv -\lim_{k_\perp \to 0} K_{\mu\nu}(k_\parallel = 0, \omega = 0). \qquad (10)$$

By combining Eqs. (9), (10) we obtain London's equation

$$\lim_{k_\perp \to 0} j_\mu(k_\parallel = 0, \omega = 0) = -D_{\mu\nu}^{(\text{s})}\lim_{k_\perp \to 0} A_\nu(k_\parallel = 0, \omega = 0) \qquad (11)$$

that captures the key features, such as the Meissner effect, of the superconducting state. $\rho_{\mu\nu}^{(\text{s})}$ is directly proportional to $D_{\mu\nu}^{(\text{s})}$:

$$\rho_{\mu\nu}^{(\text{s})} = \frac{\hbar^2}{e^2}D_{\mu\nu}^{(\text{s})} \qquad (12)$$

Notice that Eq. (11) was obtained requiring $\omega = 0$, $k_\parallel = 0$, and then taking the limit $k_\perp \to 0$. As a consequence Eq. (11) cannot be used to relate a time-dependent current to a time-dependent vector potential. This can only be done by allowing $\omega \neq 0$ when calculating $K_{\mu\nu}(\mathbf{k},\omega)$. The value of $K_{\mu\nu}(\mathbf{k},\omega)$ in the limit ($\mathbf{k} = 0, \omega \to 0$) is proportional to the Drude weight [91; 92] (see Sec. II).

For an isolated parabolic band, at zero temperature, $\rho_{\mu\nu}^{(\text{s})} = \hbar^2(n/m^*)\delta_{\mu\nu}$ [91; 92], where n is the electron density, and m^* is the effective mass of the band. This conventional result would lead us to the conclusion that for systems like MAT-BLG, for which $m^* \to \infty$, $\rho_{\mu\nu}^{(\text{s})}$ should be very small so that the hallmark signatures of superconductivity such as the Meissner effect (for 3D systems) should be extremely weak. This is in contrast with the experimental observations and shows that the conventional expression for $\rho_{\mu\nu}^{(\text{s})}$ obtained for a single parabolic band is not general enough.

For the case of a multi-band system we need to derive the expression of $\rho_{\mu\nu}^{(\text{s})}$ from the general expression of $K_{\mu\nu}(\mathbf{k},\omega)$. Using the Kubo formula we have:

$$K_{\mu\nu}(\mathbf{k},\omega) = \langle T_{\mu\nu}\rangle + \langle\chi_{\mu\nu}^p(\mathbf{k},\omega)\rangle \qquad (13)$$

where $T_{\mu\nu}$ is the diamagnetic current operator

$$T_{\mu\nu} = \sum_\sigma \int \frac{d\mathbf{k}}{(2\pi)^d}c_{\mathbf{k}\sigma}^\dagger \partial_\mu\partial_\nu H(\mathbf{k},\sigma)c_{\mathbf{k}\sigma}, \qquad (14)$$

and

$$\chi_{\mu\nu}^p(\mathbf{k},\omega) = -i\int_0^\infty dt e^{i\omega^+ t}\langle[j_\mu^p(\mathbf{k},t), j_\nu^p(-\mathbf{k},0)]\rangle \qquad (15)$$

is the time Fourier transform of the correlator of the paramagnetic current operator

$$j_\mu^p(\mathbf{k}) = \sum_\sigma \int \frac{d\mathbf{k}}{(2\pi)^d}c_{\mathbf{k}'\sigma}^\dagger \partial_\mu H(\mathbf{k}'+\mathbf{k}/2,\sigma)c_{\mathbf{k}'+\mathbf{k}\sigma}. \qquad (16)$$

The angle brackets denote expectation values over the ground state, and $[,]$ is the commutator. In Eq. (14), (16) $c_{\mathbf{k}'\sigma}^\dagger$ ($c_{\mathbf{k}'\sigma}$)

is the creation (annihilation) operator for an electron with momentum $\mathbf{k}$ and spin σ, and d is the dimensionality of the system. H is the matrix Hamiltonian describing the system expressed in the basis used for the creation annihilation operators (spin-momentum basis).

A superconductor can be described in general by a Bogolyubov de Gennes Hamiltonian $\mathcal{H}_{\mathrm{BdG}}$ of the form:

$$\mathcal{H}_{\mathrm{BdG}} = (\psi_T^\dagger \psi_B) H_{\mathrm{BdG}} \begin{pmatrix} \psi_T \\ \psi_B^\dagger \end{pmatrix}, \quad H_{\mathrm{BdG}} = \begin{pmatrix} H_T & \hat{\Delta} \\ \hat{\Delta}^\dagger & -H_B \end{pmatrix} \tag{17}$$

where $\psi_T^\dagger$, $\psi_B^\dagger$ (ψ_T, ψ_B) are the creation (annihilation) spinor operators for the states, described in the normal phase by the matrix Hamiltonians H_T, H_B, respectively, that pair to form the condensate characterized by the pairing matrix $\hat{\Delta}$. Using the expression of H_{BdG} given in Eq. (17), for $\langle T_{\mu\nu} \rangle$, in the Matsubara formalism, we obtain:

$$\langle T_{\mu\nu} \rangle = \frac{1}{\beta} \int \frac{d\mathbf{k}}{(2\pi)^d} \sum_{\omega_n} \mathrm{Tr}[\partial_\mu \partial_\nu H_{\mathrm{BdG}} G(i\omega_n, \mathbf{k})] \tag{18}$$

where $\omega_n = \pi k_B T(2n+1)$, with $n \in \mathbb{Z}$, are the fermionic Matsubara frequencies and

$$G(i\omega_n, \mathbf{k}) = [i\omega_n - H_{\mathrm{BdG}}]^{-1} = \sum_j \frac{|\psi_j(\mathbf{k})\rangle \langle \psi_j(\mathbf{k})|}{i\omega_n - E_j(\mathbf{k})} \tag{19}$$

is the retarded Green's function. In Eq. (19) E_j and $|\psi_j(\mathbf{k})\rangle$ are the eigenvalues and eigenvectors, respectively, of H_{BdG}. By performing the integration over $\mathbf{k}$ by parts, and considering that, from the definition of G, $\partial_\mu G = -G^2 \partial_\mu H_{\mathrm{BdG}}$, we can rewrite Eq. (18) in the form:

$$\langle T_{\mu\nu} \rangle = \frac{1}{\beta} \int \frac{d\mathbf{k}}{(2\pi)^d} \sum_{\omega_n} \mathrm{Tr}[\partial_\mu H_{\mathrm{BdG}} G^2(i\omega_n, \mathbf{k}) \partial_\nu H_{\mathrm{BdG}}]. \tag{20}$$

Similarly for the contribution arising from the paramagnetic currents we obtain:

$$\langle \chi_{\mu\nu}^p(\mathbf{k}, i\Omega_m) \rangle = \frac{1}{\beta} \int \frac{d\mathbf{k}'}{(2\pi)^d} \sum_{\omega_n} \mathrm{Tr}[G(i\omega_n, \mathbf{k}')$$
$$\partial_\nu H_{\mathrm{BdG}}(\mathbf{k}' + \mathbf{k}/2)\tau_z G(i\omega_n + i\Omega_m, \mathbf{k}' + \mathbf{k})$$
$$\partial_\mu H_{\mathrm{BdG}}(\mathbf{k}' + \mathbf{k}/2)\tau_z]. \tag{21}$$

where $\Omega_m = 2\pi m k_B T$ ($m \in \mathbb{Z}$) are the bosonic Matsubara frequencies, and τ_z is the z-Pauli matrix. Combining Eqs. (13), (19), (20), and (21), after summing over the fermionic Matsubara frequencies, in the limit $i\Omega_m = 0$, $\mathbf{k} \to 0$, we obtain [84]:

$$\rho_{\mu\nu}^{(s)} = \sum_{i,j} \int \frac{d\mathbf{k}}{(2\pi)^d} \frac{n_F(E_i) - n_F(E_j)}{E_j - E_i}$$
$$[\langle \psi_i | \partial_\mu H_{\mathrm{BdG}} | \psi_j \rangle \langle \psi_j | \partial_\nu H_{\mathrm{BdG}} | \psi_i \rangle$$
$$- \langle \psi_i | \partial_\mu H_{\mathrm{BdG}} \tau_z | \psi_j \rangle \langle \psi_j | \tau_z \partial_\nu H_{\mathrm{BdG}} | \psi_i \rangle] \tag{22}$$

where $n_F(E)$ is the Fermi-Dirac function.

Equation (22) can be used to show the connection between $\rho_{\mu\nu}^{(s)}$ and the quantum metric of the Bloch states. The origin of such connection can be understood by considering that in general, for a generic Hamiltonian H, the expectation values $\langle \psi_i | \partial_\mu H | \psi_j \rangle$ of the velocity operator $\partial_\mu H$ have an anomalous contribution proportional to $\langle \psi_i | \partial_\mu \psi_j \rangle$, and that therefore the terms $\langle \psi_i | \partial_\mu H_{\mathrm{BdG}} | \psi_j \rangle \langle \psi_j | \partial_\nu H_{\mathrm{BdG}} | \psi_i \rangle$ in Eq. (22) give rise to terms of the form $\langle \partial_\mu \psi_i | \partial_\nu \psi_i \rangle$ that, as shown above, Eq. (2), (4), enter the expression of the quantum metric. We call the part of $\rho_{\mu\nu}^{(s)}$ arising from these terms the "geometric part", $\rho_{\mu\nu}^{(s,\mathrm{geo})}$, of $\rho_{\mu\nu}^{(s)}$.

We can explicitly separate the contribution to $\rho_{\mu\nu}^{(s)}$ arising from the metric of the quantum states from the conventional one, arising from terms proportional to the derivatives of the eigenvalues with respect to $\mathbf{k}$. Let $\{\epsilon_{m_T}^{(T)}\}$ ($\{\epsilon_{m_B}^{(B)}\}$), $\{|m_T\rangle\}$ ($\{|m_B\rangle\}$) be the eigenvalues and eigenstates, respectively, of H_T (H_B). The Hilbert space for H_{BdG} is given by the direct sum of the Hilbert spaces $\mathcal{H}_\mathcal{T}$ of H_T and $\mathcal{H}_\mathcal{B}$ of H_B. Any eigenstate $|\psi_i\rangle$ of H_{BdG} can be written as $(|\psi_i^T\rangle, |\psi_i^B\rangle)$ with $(|\psi_i^T\rangle) \in \mathcal{H}_\mathcal{T}$, and $(|\psi_i^B\rangle) \in \mathcal{H}_\mathcal{B}$. Assuming $\hat{\Delta}$ to be independent of $\mathbf{k}$, following [84], we can rewrite Eq. (22) to identify the contribution to $\rho_{\mu\nu}^{(s)}$ arising from the quantum metric of the $|m_T\rangle$, $|m_B\rangle$ states, i.e. the quantum metric of the bands in the normal phase. To do this we start by rewriting the expectation values $\langle \psi_i | \partial_\mu H_{\mathrm{BdG}} | \psi_j \rangle$ in terms of the $|m_T\rangle$, $|m_B\rangle$ states

$$\langle \psi_i | \partial_\mu H_{\mathrm{BdG}} | \psi_j \rangle = \sum_{\substack{m_T, m_B \\ n_T, n_B}} [c_{i,m_T}^T J_{\mu,m_T,n_T}^T c_{n_T,j}^T -$$
$$c_{i,m_B}^B J_{\mu,m_B,n_B}^B c_{n_B,j}^B] \tag{23}$$

where

$$c_{i,m_X}^X = \langle \psi_i^X | m_X \rangle; \tag{24}$$
$$J_{\mu,m_X,n_X}^X = \langle m_X | \partial_\mu H_{\mathrm{BdG}} | n_X \rangle. \tag{25}$$

and $X = (T, B)$. To simplify the notation in Eqs. (23)-(25) we do not show explicitly the dependence of the quantities on the momentum $\mathbf{k}$. Using Eqs. (23)-(25) we can rewrite Eq. (22) in the form

$$\rho_{\mu\mu}^{(s)} = -4 \sum_{\substack{m_T, n_T \\ p_B, q_B, i, j}} \int \frac{d\mathbf{k}'}{(2\pi)^d} \mathrm{Re} \left[\frac{n_F(E_i) - n_F(E_j)}{E_j - E_i} \right.$$
$$\left. c_{i,m_T}^T (c_{j,n_T}^T)^* c_{j,p_B}^B (c_{i,q_B}^B)^* J_{\mu,m_T,n_T}^T J_{\mu,p_B,q_B}^B \right] \tag{26}$$

The current expectation values J_{μ,m_X,n_X}^X can be written as

$$J_{\mu,m_X,n_X}^X = \partial_\mu \epsilon_{m_X}^{(X)} \delta_{m_X,n_X} + (\epsilon_{n_X}^{(X)} - \epsilon_{m_X}^{(X)}) \langle m_X | \partial_\mu n_X \rangle. \tag{27}$$

Equation (27) shows that J_{μ,m_X,n_X}^X has a "conventional" contribution proportional to $\partial_\mu \epsilon_{m_X}^{(X)}$, and a contribution, the second term in Eq. (27), related to the geometry of the quantum states. Combining Eq. (26) and Eq. (27) we can then identify

three contributions to $\rho_{\mu\nu}^{(s)} = \rho_{\mu\nu}^{(s,1)} + \rho_{\mu\nu}^{(s,2)} + \rho_{\mu\nu}^{(s,3)}$,

$$\rho_{\mu\nu}^{(s,1)} = -4 \sum_{\substack{m_T, n_T \\ p_B, q_B, i, j}} \int \frac{d\mathbf{k}}{(2\pi)^d} \mathrm{Re}\left[C_{m_T n_T}^{p_B q_B} \partial_\mu \epsilon_{m_T}^{(T)} \partial_\nu \epsilon_{q_B}^{(B)} \delta_{m_T n_T} \delta_{p_B q_B} \right] \tag{28}$$

$$\rho_{\mu\nu}^{(s,2)} = -4 \sum_{\substack{m_T, n_T \\ p_B, q_B, i, j}} \int \frac{d\mathbf{k}}{(2\pi)^d} \mathrm{Re}\left[C_{m_T n_T}^{p_B q_B} [\partial_\mu \epsilon_{m_T}^{(T)} \delta_{m_T n_T} \right.$$
$$(\epsilon_{q_B}^{(B)} - \epsilon_{p_B}^{(B)})\langle p_B | \partial_\mu q_B\rangle$$
$$\left. + \partial_\nu \epsilon_{p_B}^{(B)} \delta_{p_B q_B} (\epsilon_{n_T}^{(T)} - \epsilon_{m_T}^{(T)})\langle m_T | \partial_\nu n_T\rangle] \right] \tag{29}$$

$$\rho_{\mu\nu}^{(s,3)} = -4 \sum_{\substack{m_T \neq n_T \\ p_B \neq q_B, i, j}} \int \frac{d\mathbf{k}}{(2\pi)^d} \mathrm{Re}\left[C_{m_T n_T}^{p_B q_B} [(\epsilon_{q_B}^{(B)} - \epsilon_{p_B}^{(B)})(\epsilon_{n_T}^{(T)} - \epsilon_{m_T}^{(T)}) \right.$$
$$\left. \langle p_B | \partial_\mu q_B\rangle \langle m_T | \partial_\nu n_T\rangle] \right]. \tag{30}$$

where

$$C_{m_T n_T}^{p_B q_B} \equiv \sum_{ij} \frac{n_F(E_i) - n_F(E_j)}{E_j - E_i} c_{i,m_T}^T (c_{j,n_T}^T)^* c_{j,p_B}^B (c_{i,q_B}^B)^*. \tag{31}$$

$\rho_{\mu\nu}^{(s,1)}$ is the conventional contribution to $\rho_{\mu\nu}^{(s)}$. $\rho_{\mu\nu}^{(s,2)}$ is a "mixed" contribution: it depends in part on the properties of the band dispersion, as the conventional part, and in part on the geometry of the quantum states. For systems with particle-hole symmetry this term is negligible. $\rho_{\mu\nu}^{(s,3)}$ has only terms proportional to $\langle m_T | \partial_\nu n_T\rangle$, i.e. terms that depend on the metric properties of the quantum states; there are no terms proportional to the gradient of the eigenvalues with respect to $\mathbf{k}$. For this reason, it is natural to identify $\rho_{\mu\nu}^{(s,3)}$ as the dominant geometric term. $\rho_{\mu\nu}^{(s)}$ and $\rho_{\mu\nu}^{(s,1)}$ are gauge invariant and therefore the combination $\rho_{\mu\nu}^{(s,2)} + \rho_{\mu\nu}^{(s,3)}$ is also gauge invariant. For this reason it is useful at times to separate $\rho_{\mu\nu}^{(s)}$ in the two terms: $\rho_{\mu\nu}^{(s,1)}$ that only depends on the bands' dispersion, and $\rho_{\mu\nu}^{(s,2)} + \rho_{\mu\nu}^{(s,3)}$ that is mostly given by the metric properties of the Bloch states. In the remainder, considering that we mostly focus on superconducting systems for which $\rho_{\mu\nu}^{(s,2)}$ is negligible, we identify $\rho_{\mu\nu}^{(s,3)}$ as the geometric part, $\rho_{\mu\nu}^{(s,\mathrm{geo})}$, of $\rho_{\mu\nu}^{(s)}$.

The expression of $\rho_{\mu\nu}^{(s,\mathrm{geo})} \equiv \rho_{\mu\nu}^{(s,3)}$ given by Eq. (30), as long as the order parameter is independent of momentum, is quite general and therefore shows the general nature of the connection between quantum metric and superfluid density. It is fairly straightforward to write a similar equations for the spin stiffness of a XY ferromagnet or the pseudo-spin stiffness of an XY orbital-ferromagnet, i.e., a state in which the degree of freedom ordering is not the spin but an orbital degree of freedom, situation that appears to be very relevant for systems like MATBLG [9; 93–95].

It is instructive to see how Eqs. (28), (30) simplify when the chemical potential lies within a well isolated band, j. In this case, neglecting terms of order $1/\Gamma_{ij}$, where $\{\Gamma_{ij}\}$ are the gaps between band j and the other bands, and assuming the pairing matrix to be proportional to the identity with amplitude Δ, we can obtain a direct relation between $\rho_{\mu\nu}^{(s,\mathrm{geo})}$ and the quantum metric $g_{\mu\nu}^{(j)}$ of band j when time-reversal symmetry is preserved and the superconducting order parameter, in addition to being $\mathbf{k}$-independent, only has intraband terms. In this case we have [84]:

$$\rho_{\mu\nu}^{(s)} = \int \frac{d\mathbf{k}}{(2\pi)^d} \left[2\frac{\partial n_F(E_j)}{\partial E_j} + \frac{1 - 2n_F(E_j)}{E_j} \right] \frac{\Delta^2}{E_j^2} \partial_\mu \epsilon_j \partial_\nu \epsilon_j +$$
$$2\Delta^2 \int \frac{d\mathbf{k}}{(2\pi)^d} \frac{1 - 2n_F(E_j)}{E_j} g_{\mu\nu}^{(j)} \tag{32}$$

where $\mathbf{k}$ is the momentum. The last term in Eq (32) is the geometric part of $\rho_{\mu\nu}^{(s)}$ that, in this simple case, is related in a very direct way to the quantum metric $g_{\mu\nu}^{(j)}$ of the isolated band.

Using the expression above, and the inequality (6) *for the case of an isolated band* we can provide a bound for the geometric part of $\rho_{\mu\nu}^{(s)}$ [82; 84]:

$$\rho^{(s,\mathrm{geo})\mu\nu} \geq 2\Delta^2 \int \frac{d\mathbf{k}}{(2\pi)^d} \frac{1 - 2n_F(E_j)}{E_j} |B_{\mu\nu}|^2. \tag{33}$$

This result shows that for bands with large Berry curvature the geometric contribution to $\rho_{\mu\nu}^{(s)}$ is large. It is important to point out that Eq. (33) only provides a lower bound given that it is possible to have situations in which $g_{\mu\nu} \neq 0$ even if the Berry curvature is zero [75].

In 2D, for the case in which the isolated band, is flat, i.e. having a bandwidth much smaller than the Γ_{ij} gaps, and *non degenerate*, $\rho_{\mu\nu}^{(s)}$ is only given by the geometric part and can be written in the form [82]:

$$\rho_{\mu\nu}^{(s)} = 2\Delta\sqrt{\nu(1-\nu)} \int \frac{d\mathbf{k}}{(2\pi)^2} g_{\mu\nu}(\mathbf{k}). \tag{34}$$

where ν is the filling fraction of the flat band. In this case we have that $(1/2\pi)\int d\mathbf{k} B_{\mu\nu} = \varepsilon_{\mu\nu} C$, where $\varepsilon_{\mu\nu}$ is the 2×2 Levi-Civita tensor and C is the Chern number of the isolated band. Using inequality (5) we obtain $\det(\int d\mathbf{k} g_{\mu\nu}) \geq \det(d\mathbf{k} \int |B_{\mu\nu}|^2 = C^2$ and then, for an isotropic system [82]:

$$\rho^{(s)} \geq \frac{\Delta}{\pi}\sqrt{\nu(1-\nu)}|C|. \tag{35}$$

In general, when the 2D flat band has degenerate points it might not be possible to find a lower bound for $\rho_{\mu\nu}^{(s)} = \rho_{\mu\nu}^{(s,\mathrm{geo})}$, however, this can be done for the case relevant to MATBLG in which the two low-energy 2D flat band have degeneracy points and $C_{2z}\mathcal{T}$ symmetry, C_{2z} being the twofold rotation around the z-axis perpendicular to the 2D plane to which the quantum states are confined, and $\mathcal{T}$ the time-reversal operator [96]. Given the degeneracy of the bands it is necessary to consider the non-Abelian generalization of the expression of $Q_{\mu\nu}$. It can be shown that the $C_{2z}T$ symmetry constrains the non-Abelian Berry curvature to the form [97; 98] $B_{xy} = -b_{xy}(\mathbf{k})\sigma_2$ with $(1/2\pi)\int d\mathbf{k} b_{xy} = e_2$, where e_2 is the Wilson loop winding number [97], or "Euler's class" [98],

of the two bands. In this case, assuming the pairing Δ is non vanishing only for the low-energy, two-fold degenerate, band, and using again inequality (6), we have that $\rho^{(s)}$ has the lower bound [96]

$$\rho^{(s)} \geq \frac{\Delta}{\pi}\sqrt{\nu(1-\nu)}|e_2|. \qquad (36)$$

For the specific case of TBLG $e_2 = 1$ so that, taking into account the spin and valley degeneracy, we obtain [96]

$$\rho^{(s)} \geq 4\frac{\Delta}{\pi}\sqrt{\nu(1-\nu)}. \qquad (37)$$

Inequalities (35), (36) show how the topological invariants of the bands can be used to obtain lower bounds for $\rho_{\mu\nu}^{(s)}$ in flat-band systems.

For a superconductor $\rho_{\mu\nu}^{(s)}$ determines the phase-stiffness of the superconducting state and therefore its stability against fluctuations. $\rho_{\mu\nu}^{(s)}$ also determines the superfluid density, a quantity that can be measured directly.

$\rho^{(s)} = \rho_s = (1/d)\text{Tr}\rho_{\mu\nu}^{(s)}$ is easy to measure for 3D superconductors, given that it is related to to the London penetration depth λ_L via the equation

$$\lambda_L = \frac{\hbar}{e}\frac{1}{\sqrt{\mu_0\rho_s}} \qquad (38)$$

where μ_0 is the magnetic permeability.

For 2D superconductors ρ_s cannot be obtained indirectly by measuring λ_L and recently techniques have been proposed to obtain it via a direct measurement [99]. However, for 2D superconductors, and in general 2D ground states that break a U(1) symmetry, $\rho^{(s)}$ can also be obtained experimentally via Eq. (8) relating T_{KT} to $\rho^{(s)}$. In particular, for 2D superconductors, T_{KT} can be obtained as the temperature at which the voltage V across the superconductor scales as I^3, I being the current. This was the approach used in Ref. [7] to estimate T_{KT} in MATBLG. Using Eqs. (8) and (22) we can relate T_{KT} to ρ_s. This requires to properly take into account the temperature dependence of ρ_s: in addition to the temperature dependence due to the presence of the Fermi occupation factors, we must include the temperature dependence of the order parameter Δ. For many of the second-order phase transitions of interest, in first approximation, we can assume the "BCS scaling" $\Delta(T) = 1.76k_B(1 - T/T_c)^{1/2}$. In general $\Delta(T)$ can be obtained by solving the non-linear gap equation. For the concrete example of superconducting MATBLG discussed in Sec. IV we have found that the BCS scaling of $\Delta(T)$ agrees well with the one obtained solving the non-linear gap equation.

IV. QUANTUM METRIC EFFECTS FOR CORRELATED STATES IN TWISTED BILAYER GRAPHENE

The behavior of TBLG is particularly interesting for twist angles $\theta \sim 1.00°$. For such small twist angles the moiré primitive cell is very large and the most effective way to obtain the electronic structure is to use an effective low-energy continuum model [19]. The details of the model can be found in Ref. [19], here we briefly outline the model's essential elements and assumptions. In graphene the conduction and valence bands cross at the corners $\mathbf{K}$ of the hexagonal Brillouin zone (BZ), $|\mathbf{K}| = 4\pi/3a_0$ with a_0 the graphene's carbon-carbon distance. Around the $\mathbf{K}$ points electrons in graphene behave as massless Dirac fermions [100] and the Hamiltonian for each layer, top (t) and bottom (b), forming TBLG is

$$H_{t/b} = v_F\mathbf{k}_{t/b} \cdot \boldsymbol{\sigma} - \mu\sigma_0, \qquad (39)$$

where $v_F = 10^6$ m/s is graphene's Fermi velocity, $\mathbf{k}_{t/b} = (k_x, k_y)_{t/b}$ is the 2D momentum, measured from the $\mathbf{K}_{t/b}$ point, for an electron in the top/bottom layer, $\boldsymbol{\sigma} = (\sigma_x, \sigma_y)$ is the 2D vector formed by the x, y Pauli matrices in sublattice space [100], μ is the chemical potential, and σ_0 is the 2×2 identity matrix. Conservation of crystal momentum requires $\mathbf{k}_b = \mathbf{k}_t + (\mathbf{K}_t - \mathbf{K}_b) + (\mathbf{G}_t - \mathbf{G}_b)$. Here $\{\mathbf{G}_{t/b}\}$ are the reciprocal lattice wave vectors in the top/bottom layer. Due to the twist the set of $\{\mathbf{G}_t\}$ is different from the set of $\{\mathbf{G}_b\}$. In the model of Ref. [19] only the tunneling processes for which $|\mathbf{k}_b - \mathbf{k}_t| = |\mathbf{K}_t - \mathbf{K}_b| = 2K\sin(\theta/2)$, are taken into account. There are three vectors $\mathbf{Q}_i = (\mathbf{K}_t - \mathbf{K}_b) + (\mathbf{G}_t - \mathbf{G}_b)_i$ $(i = -1, 0, 1)$ for which $Q \equiv |\mathbf{Q}| = 2K\sin(\theta/2)$ to which correspond the interlayer tunneling matrices [19]

$$T_0 = w\begin{pmatrix} 1 & 1 \\ 1 & 1 \end{pmatrix}; \qquad T_{\pm 1} = w\begin{pmatrix} e^{\pm i2\pi/3} & 1 \\ e^{\mp i2\pi/3} & e^{\pm i2\pi/3} \end{pmatrix} \qquad (40)$$

where $w \approx 100$ meV is the interlayer tunneling strength. Up to an overall scale factor the bands only depend on the ratio w/v_FQ [19]. In the remainder we set $w = 118$ meV. The precise value of w depends on the detail of the experimental sample. In addition, due to corrugation effects the tunneling strength, w_0, for regions with AA stacking can be different from the one, w_1, for regions with AB stacking. We assume the ratio w_0/w_1 to be uniform and equal to 1. Changes in the ratio w_0/w_1 affect the low energy bands and therefore the superfluid stiffness. All the tunneling processes for which $|\mathbf{k}_b - \mathbf{k}_t| = Q$ are taken into account by keeping all the recursive tunneling processes on a honeycomb structure constructed in momentum space with nearest neighbor sites connected by the vectors $\mathbf{Q}_i$. The primitive cell of this structure is the moiré lattice's mini-BZ. We adopt the convention in which the corners, $\kappa_\pm$, of the mini-BZ coincide with the points for which $\mathbf{k}_{t/b} = 0$. The number of sites of the honeycomb structure in momentum space used to obtain the band structure is increased until the bands converge. We find that for $w = 118$ meV and $\theta \approx 1.00°$ convergence is reached when the number of sites is ~ 200.

In Ref. [19] and other works θ_M is defined as the twist angle for which the Fermi velocity at the $\kappa_\pm$ points of the mini-BZ vanishes, whereas in other works it is defined as the value of θ for which the bandwidth of the conduction, or valence, band is minimum. In the reminder we will adopt this second definition. Figure 1 (a) shows the 2D valence band at the magic angle $\theta = 1.05°$. We see that the bandwidth is just ~ 2 meV. Small deviations of θ away from θ_M have large effects on the

bandwidth of the lowest energy bands. This can be seen from Fig. 1 (b), showing the 2D valence band for $\theta = 1.00°$: a change of just $0.05°$ in θ results in a factor of 3 change in the bandwidth of the lowest energy bands. The change in the bandwidth, in turn, strongly affects the stability, and properties of the correlated ground states.
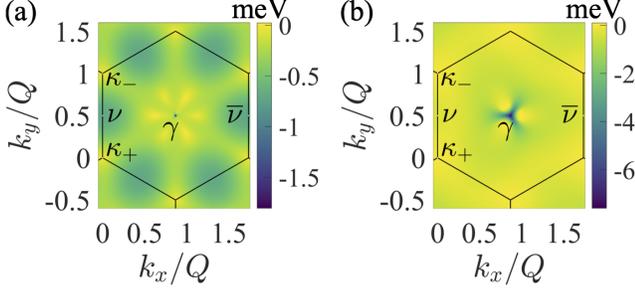
FIG. 1. Valence band of TBLG for $\theta = 1.05°$, (a), and $\theta = 1.00°$, (b). The high symmetry points in the moiré Brillouin zone (BZ) are also shown. Adapted from [101].

The superconducting paring matrix $\hat{\Delta}$ is obtained via the mean-field approximation after adding an effective local (s-wave) attractive interaction whose strength is set so that at the magic angle, $\theta = 1.05°$, $T_c = 1.63$K when $\mu = -0.3$ meV [101], in agreement with experiments [3]. $\hat{\Delta}$ describes an s-wave superconductor whose only significant Fourier components are the one with wave vector $\mathbf{q}$ equal to zero and the ones with $\mathbf{q} = \mathbf{Q}_i$ [101; 102].

The large size of the moiré primitive cell in TBLG when θ is of the order of $1°$ implies that effectively TBLG is a system with a large number of orbital degrees of freedom. This results in a very non-trivial quantum geometric tensors. In particular, for θ close to the magic angle, we have several regions of the BZ where the Berry curvature is very large. Considering that the positive semidefinite nature of $Q_{\mu\nu}$ implies $\det g_{\mu\nu} \geq |B_{\mu\nu}|^2$, see Sec. II, we expect in these regions the geometric contribution to $\rho_{\mu\nu}^{(s)}$ to be large. Fig. 2 (a) shows the profile in the BZ of the integrand to obtain $\rho_{\mu\mu}^{(s,geo)}$ for $\theta = 1.05°$. From this figure we see that at the magic angle there are large regions in the mini BZ that provide strong contributions to $\rho_{\mu\mu}^{(s,geo)}$. Figure 2 (b) shows the conventional, geometric, and total, longitudinal superfluid stiffness for different, small, values of θ and fixed μ. We see that that $\rho_{\mu\mu}^{(s,geo)}$ is larger than $\rho_{\mu\mu}^{(s,conv)}$ only close to the magic angle, but that it is significant for all the values of θ smaller than $1.1°$.

The results of Fig. 2 (b) show that systems like TBLG are an ideal playground in which to test the connection between quantum geometry and macroscopic properties of correlated ground states. This can be seen, for instance, by considering the scaling of ρ_s with the chemical potential μ at the magic angle, and away from it. The conventional contribution to $\rho_{\mu\nu}^{(s)}$, in general, increases with doping, and therefore with μ. As a consequence, in systems in which the superfluid stiffness is mostly due to the conventional term, the total ρ_s increases with μ. This is the case also for TBLG away from the magic
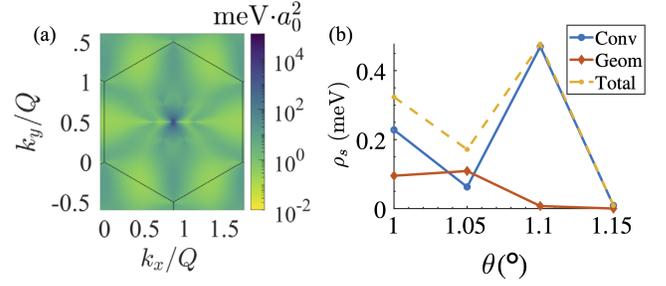
FIG. 2. (a) Integrand of $\rho_{\mu\mu}^{(s,geo)}$ for TBLG at the magic angle. $\mu = -0.30$ meV. (b) Conventional (Conv) and geometric (Geom) contributions to the total longitudinal superfluid stiffness, $\rho_s \equiv (1/2)\text{Tr}\rho_{\mu\nu}^{(s)}$, for TBLG as a function of twist angle. $\mu = -0.3$ meV. Adapted from [101].

angle as shown in Fig 3 (a) for which the conventional contribution to ρ_s is larger than the geometric contribution. The geometric contribution to $\rho_{\mu\nu}^{(s)}$, in general, can increase or decrease with doping. From Fig. 3 (a) we see that, for $\theta = 1.00°$, $\rho_{\mu\nu}^{(s,geo)}$ decreases with μ. This is also the case at the magic angle where, however, $\rho_{\mu\nu}^{(s,geo)}$ dominates over $\rho_{\mu\nu}^{(s,conv)}$. As a consequence at the magic angle we have the unusual situation that the total $\rho_{\mu\nu}^{(s)}$ decreases with μ as as shown in Fig 3 (b).
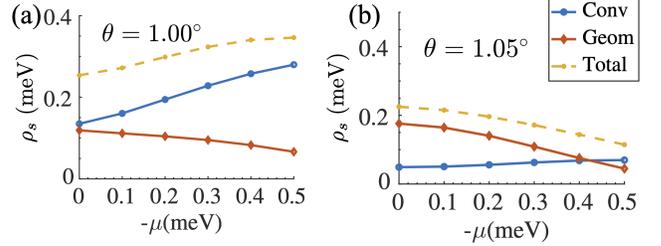
FIG. 3. Conventional (Conv) and geometric (Geom) contributions to ρ_s as a function of doping, μ (hole doping), for TBLG with $\theta = 1.00°$, (a), and $\theta = 1.05°$ (magic angle), (b). Adapted from [101].

We expect that the scalings of ρ_s with respect to μ will be reflected in the scaling of T_{KT}. Using Eq. (8), knowing the temperature scaling of $\rho_{\mu\nu}^{(s)}$, T_{KT} can be calculated. Figure 4 (a) shows the results for the ratio T_{KT}/T_c away from the magic angle, $\theta = 1.00°$. As expected we see that T_{KT}/T_c increases as the hole density increases. At the magic angle we have instead that T_{KT}/T_c decreases with doping, as shown in Fig 4 (b), a consequence of the fact that at the magic angle the geometric contribution of $\rho_{\mu\nu}^{(s)}$ dominates.

In a 2D superconductor the unbounding of the vortices due to thermal fluctuations causes a finite resistance and therefore a finite longitudinal voltage, V_{xx}, that depends on the strength of the electrical current I driven through the system. For $T = T_{KT}$ we have that $V_{xx} \propto I^3$. By measuring the $V_{xx}(I)$ relation at different temperatures is then possible to estimate T_{KT} as the temperature for which $V_{xx} \propto I^3$. For TBLG this
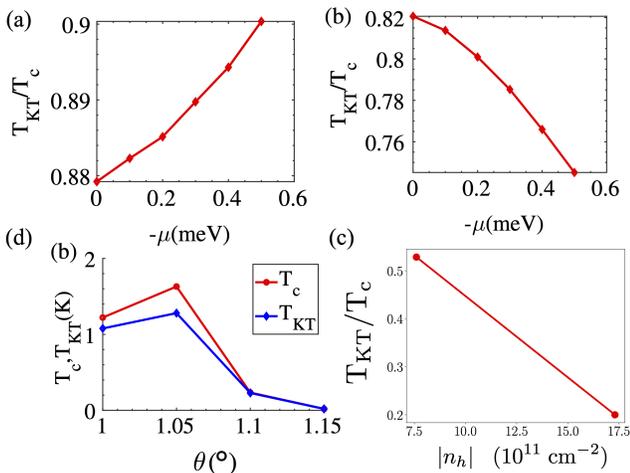
FIG. 4. Calculated T_{KT}/T_c as a function of μ for $\theta = 1.00°$, away from the magic angle, (a), and at the magic angle (b); adapted from [101]. (c) T_{KT}/T_c as a function of $|n_h|$ in the hole-doped regime obtained from the experimental measurements presented in Ref. [7]. (d) T_c and T_{KT} as a function of θ for TBLG when $\mu = -0.3$ meV; adapted from [101].

was done in Ref. [7]. Figure 4 (c) shows the scaling of T_{KT} $/T_c$ obtained using the two data points presented in the "Extended Data Table 1" of Ref. [7] for MATBLG in the hole doped regime. The figure shows that in the MATBLG samples used in Ref. [7], in the hole-doped regime, T_{KT} $/T_c$ decreases with doping in qualitative agreement with the results of Fig 4 (b), suggesting that also experimentally, in the hole-doped regime, the geometric contribution of $\rho_{\mu\nu}^{(s)}$ dominates over the conventional one.

Figure 4 (d) shows the dependence in TBLG of T_{KT} on the twist angle for fixed chemical potential, $\mu = -0.3$ meV. These results show that, because of the geometric contribution to ρ_s, at the magic angle T_{KT} is largest, along with T_c. This suggests that in multiorbital systems, like TBLG, the geometric contribution to ρ_s can compensate the suppression of $\rho_{\mu\mu}^{(s,conv)}$ associated with the flattening of the bands and lead to robust superfluid states.

The discussion above focused on the case when the correlated ground state breaking a $U(1)$ symmetry is the superconducting state. A very similar discussion can be carried out for other ground states that break a $U(1)$ symmetry. In particular similar results can be obtained for the ferromagnetic state [103–105]. Recently it has been suggested that an "orbital-magnetic" state, characterized by a non-zero sublattice polarization, might be one of the correlated states most likely realized in TBLG [9; 93–95]. Also for this state, an analysis similar to the one presented above for the superconducting state can be done.

More recently, we have considered the possibility that in double TBLG an exciton condensate state might be realized [106]. This is a long sought correlated state in which electron and holes (e-h) pair to form a neutral superfluid [107–115]. We considered a double layer formed by two MATBLG,

one electron-doped and one hole-doped, separated by a thin dielectric. As for the case of superconductivity the flatness of the bands, while favoring the formation of e-h pairs, can lead to a very small superfluid density. We found that, for the exciton condensate, the quantum metric plays an even more critical role than for the superconducting case in stabilizing the collective state and in guaranteeing a nonzero value of the superfluid stiffness [106].

V. CONCLUSIONS AND OUTLOOK

The experimental realization of magic angle twisted bilayer graphene systems has opened a completely new avenue to explore the connection between the metric of quantum states and the properties of strongly correlated states that break continuous symmetries. It has shown experimentally that the flatness of the low energy bands does not necessarily imply a low superconducting density $\rho_{\mu\nu}^{(s)}$ and demonstrated the importance of the interband contributions, associated with a non-trivial quantum metric of the bands, to $\rho_{\mu\nu}^{(s)}$.

The experimental results on MATBLG, combined with the theoretical treatment of $\rho_{\mu\nu}^{(s)}$ that includes the geometric contribution [82–84; 96; 101; 105; 116–118], show that the quantum metric plays an important role in determining the properties of the correlated states of multi-orbital systems. Multilayers formed by 2D crystals stacked with relative small twist angles have very large moiré primitive cells and therefore many orbitals and low energy bands with very small bandwidths. For these systems, therefore, the quantum metric plays in important role in determining the stability and properties of correlated ground states. We expect that the study of the connection between quantum metric and properties of correlated states will be extended to several new twisted 2D multilayers, both based on graphene [6; 119], and on other 2D crystals such as monolayers of transition metal dichalcogenides [16; 120–132].

A new interesting research direction would be the study of the interplay between quantum metric, disorder, and stiffness of the correlated states, in particular in twisted bilayers [133]. We could expect that for states like superconductivity disorder might suppress the conventional part of $\rho_{\mu\nu}^{(s)}$ more than the geometric part. It will be interesting to verify theoretically and experimentally the extent of the validity of such expectation.

Correlated states that break a continuous symmetry can differ topologically. For these states it will be interesting to investigate how the connection between quantum metric and stiffness might vary between the different topological phases, and, more in particular, if there are features of such connection that can be used to identify the topological phases. For instance, topologically different superconducting phases can be realized in superconducting quantum anomalous Hall (QAH) states [134]. Considering the recent observation of signatures of QAH states in MATBLG, superconducting topological states might be realized in MATBLG proximitized to a superconductor.

In some cases, correlated states breaking different continu-

ous symmetries can compete or coexist. It will be interesting to study the relation between quantum metric and properties such as $\rho_{\mu\nu}^{(s)}$ of competing or coexisting collective states in systems like TBLG.

As discussed in Sec. III, in 2D systems, experimental evidence of the connection between quantum metric and $\rho_{\mu\nu}^{(s)}$ can be obtained indirectly by obtaining the scaling of T_{KT} with respect to other tunable quantities such as doping. It will be interesting to have more direct experimental evidence of the effects of the metric of the quantum states on the properties of correlated states. One approach would be to measure the dispersion of the Goldstone modes associated with the spontaneous breaking of the continuous symmetry given that $\rho_{\mu\nu}^{(s)}$ enters the dispersion of such modes.

In general, the quantitative understanding of the relation between quantum metric and the stability and properties of collective ground states will allow to better design strongly interacting systems with the desired functionalities. By designing multiorbital systems with flat bands that maximize the quantum metric we can achieve both large values of T_c and superfluid density, properties that are desirable in several applications.

[1] G. Li, A. Luican, J. M. B. Lopes dos Santos, A. H. Castro Neto, A. Reina, J. Kong, and E. Y. Andrei, Observation of Van Hove singularities in twisted graphene layers, Nature Physics 6, 109 (2010), arXiv:0912.2102.

[2] K. Kim, A. DaSilva, S. Huang, B. Fallahazad, S. Larentis, T. Taniguchi, K. Watanabe, B. J. LeRoy, A. H. MacDonald, and E. Tutuc, Tunable moiré bands and strong correlations in small-twist-angle bilayer graphene, Proceedings of the National Academy of Sciences of the United States of America 114, 3364 (2017).

[3] Y. Cao, V. Fatemi, S. Fang, K. Watanabe, T. Taniguchi, E. Kaxiras, and P. Jarillo-Herrero, Unconventional superconductivity in magic-angle graphene superlattices, Nature 556, 43 (2018).

[4] Y. Cao, V. Fatemi, A. Demir, S. Fang, S. Tomarken, J. Luo, J. Sanchez-Yamagishi, K. Watanabe, T. Taniguchi, E. Kaxiras, R. Ashoori, and P. Jarillo-Herrero, Correlated insulator behaviour at half-filling in magic-angle graphene superlattices, Nature 556, 80 (2018).

[5] M. Yankowitz, S. Chen, H. Polshyn, Y. Zhang, K. Watanabe, T. Taniguchi, D. Graf, A. Young, and C. Dean, Tuning superconductivity in twisted bilayer graphene, Science 363, 1059 (2019).

[6] G. Chen, A. L. Sharpe, P. Gallagher, I. T. Rosen, E. J. Fox, L. Jiang, B. Lyu, H. Li, K. Watanabe, T. Taniguchi, J. Jung, Z. Shi, D. Goldhaber-Gordon, Y. Zhang, and F. Wang, Signatures of tunable superconductivity in a trilayer graphene moiré superlattice, Nature 572, 215 (2019).

[7] X. Lu, P. Stepanov, W. Yang, M. Xie, M. A. Aamir, I. Das, C. Urgell, K. Watanabe, T. Taniguchi, G. Zhang, A. Bachtold, A. H. MacDonald, and D. K. Efetov, Superconductors, orbital magnets and correlated states in magic-angle bilayer graphene, Nature 574, 653 (2019).

[8] Y. Choi, J. Kemmer, Y. Peng, A. Thomson, H. Arora, R. Polski, Y. Zhang, H. Ren, J. Alicea, G. Refael, T. Taniguchi, and S. Nadj-Perge, Electronic correlations in twisted bilayer graphene near the magic angle, Nature Physics 15, 1174 (2019).

[9] A. L. Sharpe, E. J. Fox, A. W. Barnard, J. Finney, K. Watanabe, T. Taniguchi, M. A. Kastner, and D. Goldhaber-Gordon, Emergent ferromagnetism near three-quarters filling in twisted bilayer graphene, Science 365, 605 (2019).

[10] H. Polshyn, M. Yankowitz, S. Chen, Y. Zhang, K. Watanabe, T. Taniguchi, C. R. Dean, and A. F. Young, Large linear-in-temperature resistivity in twisted bilayer graphene, Nature Physics 15, 1011 (2019).

[11] E. Codecido, Q. Wang, R. Koester, S. Che, H. Tian, R. Lv, S. Tran, K. Watanabe, T. Taniguchi, F. Zhang, M. Bockrath, and C. N. Lau, Correlated insulating and superconducting states in twisted bilayer graphene below the magic angle, Science Advances 5, eaaw9770 (2019).

[12] X. Liu, Z. Hao, E. Khalaf, J. Y. Lee, Y. Ronen, H. Yoo, D. Haei Najafabadi, K. Watanabe, T. Taniguchi, A. Vishwanath, and P. Kim, Tunable spin-polarized correlated states in twisted double bilayer graphene, Nature 583, 221 (2020).

[13] C. Shen, Y. Chu, Q. S. Wu, N. Li, S. Wang, Y. Zhao, J. Tang, J. Liu, J. Tian, K. Watanabe, T. Taniguchi, R. Yang, Z. Y. Meng, D. Shi, O. V. Yazyev, and G. Zhang, Correlated states in twisted double bilayer graphene, Nature Physics 16, 520 (2020).

[14] G. Chen, A. L. Sharpe, E. J. Fox, Y. H. Zhang, S. Wang, L. Jiang, B. Lyu, H. Li, K. Watanabe, T. Taniguchi, Z. Shi, T. Senthil, D. Goldhaber-Gordon, Y. Zhang, and F. Wang, Tunable correlated Chern insulator and ferromagnetism in a moiré superlattice, Nature 579, 56 (2020).

[15] Y. Cao, D. Rodan-Legrain, O. Rubies-Bigorda, J. M. Park, K. Watanabe, T. Taniguchi, and P. Jarillo-Herrero, Tunable correlated states and spin-polarized phases in twisted bilayer-bilayer graphene, Nature 583, 215 (2020).

[16] L. Wang, E.-M. Shih, A. Ghiotto, L. Xian, D. A. Rhodes, C. Tan, M. Claassen, D. M. Kennes, Y. Bai, B. Kim, K. Watanabe, T. Taniguchi, X. Zhu, J. Hone, A. Rubio, A. N. Pasupathy, and C. R. Dean, Correlated electronic phases in twisted bilayer transition metal dichalcogenides, Nature Materials 19, 861 (2020).

[17] J. M. B. Lopes dos Santos, N. M. R. Peres, and A. H. Castro Neto, Graphene bilayer with a twist: Electronic structure, Phys. Rev. Lett. 99, 256802 (2007).

[18] E. Suárez Morell, J. D. Correa, P. Vargas, M. Pacheco, and Z. Barticevic, Flat bands in slightly twisted bilayer graphene

: Tight-binding calculations, Phys. Rev. B **82**, 121407(R) (2010).

[19] R. Bistritzer and A. H. MacDonald, Moire bands in twisted double-layer graphene, Proc. National Acad. Sciences United States Am. **108**, 12233 (2011).

[20] J. P. Provost and G. Vallee, Riemannian structure on manifolds of quantum states, Communications in Mathematical Physics **76**, 289 (1980).

[21] D. N. Page, Geometrical description of Berry's phase, Physical Review A **36**, 3479 (1987).

[22] I. Bengtsson and K. Zyczkowski, *Geometry of Quantum States: An Introduction to Quantum Entanglement* (Cambridge University Press, Cambridge, 2017) pp. 1–619.

[23] R. Cheng, Quantum geometric tensor (fubini-study metric) in quantum system: A pedagogical introduction, arXiv:1012.1337 (2010).

[24] M. V. Berry, Quantal phase factors accompanying adiabatic changes, Proceedings of the Royal Society of London. A. Mathematical and Physical Sciences **392**, 45 (1984).

[25] N. Read and D. Green, Paired states of fermions in two dimensions with breaking of parity and time-reversal symmetries and the fractional quantum hall effect, Phys. Rev. B **61**, 10267 (2000).

[26] A. P. Schnyder, S. Ryu, A. Furusaki, and A. W. W. Ludwig, Classification of topological insulators and superconductors in three spatial dimensions, Phys. Rev. B **78**, 195125 (2008).

[27] M. Z. Hasan and C. L. Kane, Colloquium: Topological Insulators, Rev. Mod. Phys. **82**, 3045 (2010).

[28] X.-L. Qi and S.-C. Zhang, Topological insulators and superconductors, Rev. Mod. Phys. **83**, 1057 (2011).

[29] C.-K. Chiu, J. C. Y. Teo, A. P. Schnyder, and S. Ryu, Classification of topological quantum matter with symmetries, Reviews of Modern Physics **88**, 035005 (2016).

[30] T. Wehling, A. Black-Schaffer, and A. Balatsky, Dirac materials, Advances in Physics **63**, 1 (2014).

[31] O. Vafek and A. Vishwanath, Dirac fermions in solids: From high-T_c cuprates and graphene to topological insulators and Weyl semimetals, Annual Review of Condensed Matter Physics **5**, 83 (2014).

[32] N. P. Armitage, E. J. Mele, and A. Vishwanath, Weyl and Dirac semimetals in three-dimensional solids, Reviews of Modern Physics **90**, 015001 (2018).

[33] A. A. Burkov, Weyl Metals, Annual Review of Condensed Matter Physics **9**, 359 (2018).

[34] W. A. Benalcazar, B. A. Bernevig, and T. L. Hughes, Quantized electric multipole insulators, Science **357**, 61 (2017).

[35] F. Schindler, A. M. Cook, M. G. Vergniory, Z. Wang, S. S. P. Parkin, B. A. Bernevig, and T. Neupert, Higher-order topological insulators, Science Advances **4**, eaat0346 (2018).

[36] Z. Song, Z. Fang, and C. Fang, Dimensional edge states of rotation symmetry protected topological states, Physical Review Letters **119**, 246402 (2017).

[37] E. Khalaf, Higher-order topological insulators and superconductors protected by inversion symmetry, Physical Review B **97**, 205136 (2018).

[38] M. Ezawa, Minimal models for Wannier-type higher-order topological insulators and phosphorene, Physical Review B **98**, 045125 (2018).

[39] L. Trifunovic and P. W. Brouwer, Higher-Order Bulk-Boundary Correspondence for Topological Crystalline Phases, Physical Review X **9**, 011012 (2019).

[40] S. A. A. Ghorashi, X. Hu, T. L. Hughes, and E. Rossi, Second-order Dirac superconductors and magnetic field induced Majorana hinge modes, Physical Review B **100**, 020509 (2019),

arXiv:1901.07579.

[41] S. A. A. Ghorashi, T. L. Hughes, and E. Rossi, Vortex and Surface Phase Transitions in Superconducting Higher-order Topological Insulators, Physical Review Letters **125**, 037001 (2020), arXiv:1909.10536.

[42] Y. Fang and J. Cano, Higher-order topological insulators in antiperovskites, Physical Review B **101**, 245110 (2020).

[43] T. Kibble, Geometrization of quantum mechanics, Communications in Mathematical Physics **65**, 189 (1979).

[44] A. Ashtekar and T. A. Schilling, Geometrical Formulation of Quantum Mechanics, in *On Einstein's Path* (Springer New York, New York, NY, 1999) pp. 23–65.

[45] G. Fubini, Sulle metriche definite da una forma hermitiana, Atti del Reale Istituto Veneto di Scienze, Lettere ed Arti **63**, 502 (1904).

[46] E. Study, Kürzeste Wege im komplexen Gebiet, Mathematische Annalen **60**, 321 (1905).

[47] R. Roy, Band geometry of fractional topological insulators, Physical Review B **90**, 165139 (2014).

[48] Y.-Q. Ma, S. Chen, H. Fan, and W.-M. Liu, Abelian and non-Abelian quantum geometric tensor, Physical Review B **81**, 245129 (2010), arXiv:1003.4040.

[49] F. Wilczek and A. Zee, Appearance of gauge structure in simple dynamical systems, Physical Review Letters **52**, 2111 (1984).

[50] D. Xiao, M. C. Chang, and Q. Niu, Berry phase effects on electronic properties, Reviews of Modern Physics **82**, 1959 (2010), arXiv:0907.2021.

[51] B. A. Bernevig and T. L. Hughes, *Topological insulators and topological superconductors* (Princeton University Press, 2013).

[52] J. E. Avron, R. Seiler, and P. G. Zograf, Viscosity of quantum hall fluids, Physical Review Letters **75**, 697 (1995), arXiv:9502011 [cond-mat].

[53] N. Read, Non-Abelian adiabatic statistics and Hall viscosity in quantum Hall states and px + ipy paired superfluids, Physical Review B - Condensed Matter and Materials Physics **79**, 1 (2009), arXiv:0805.2507.

[54] F. D. M. Haldane, "Hall viscosity" and intrinsic metric of incompressible fractional Hall fluids, arXiv:0906.1854 (2009), arXiv:0906.1854.

[55] N. Read and E. H. Rezayi, Hall viscosity, orbital spin, and geometry: Paired superfluids and quantum Hall systems, Physical Review B - Condensed Matter and Materials Physics **84**, 1 (2011), arXiv:1008.0210.

[56] C. Hoyos and D. T. Son, Hall Viscosity and Electromagnetic Response, Physical Review Letters **108**, 066805 (2012).

[57] B. Bradlyn, M. Goldstein, and N. Read, Kubo formulas for viscosity: Hall viscosity, Ward identities, and the relation with conductivity, Physical Review B **86**, 245309 (2012).

[58] F. D. M. Haldane and Y. Shen, Geometry of Landau orbits in the absence of rotational symmetry, arXiv:1512.04502 (2015), arXiv:1512.04502.

[59] H. Shapourian, T. L. Hughes, and S. Ryu, Viscoelastic response of topological tight-binding models in two and three dimensions, Physical Review B **92**, 165131 (2015), arXiv:1505.03868.

[60] T. Holder, R. Queiroz, and A. Stern, Unified description of the classical hall viscosity, Physical Review Letters **123**, 106801 (2019), arXiv:1903.05541.

[61] T. L. Hughes, R. G. Leigh, and E. Fradkin, Torsional Response and Dissipationless Viscosity in Topological Insulators, Physical Review Letters **107**, 075502 (2011), arXiv:1101.3541.

[62] L. V. Delacrétaz and A. Gromov, Transport Signatures of the Hall Viscosity, Physical Review Letters **119**, 226602 (2017), arXiv:1706.03773.

[63] T. Scaffidi, N. Nandi, B. Schmidt, A. P. Mackenzie, and J. E. Moore, Hydrodynamic Electron Flow and Hall Viscosity, Physical Review Letters **118**, 226601 (2017), arXiv:1703.07325.

[64] F. M. D. Pellegrino, I. Torre, and M. Polini, Nonlocal transport and the Hall viscosity of two-dimensional hydrodynamic electron liquids, Physical Review B **96**, 195401 (2017).

[65] A. I. Berdyugin, S. G. Xu, F. M. D. Pellegrino, R. Krishna Kumar, A. Principi, I. Torre, M. Ben Shalom, T. Taniguchi, K. Watanabe, I. V. Grigorieva, M. Polini, A. K. Geim, and D. A. Bandurin, Measuring Hall viscosity of graphene's electron fluid, Science **364**, eaau0685 (2019).

[66] P. Rao and B. Bradlyn, Hall Viscosity in Quantum Systems with Discrete Symmetry: Point Group and Lattice Anisotropy, Physical Review X **10**, 021005 (2020), arXiv:1910.10727.

[67] A. Gianfrate, O. Bleu, L. Dominici, V. Ardizzone, M. De Giorgi, D. Ballarini, G. Lerario, K. W. West, L. N. Pfeiffer, D. D. Solnyshkov, D. Sanvitto, and G. Malpuech, Measurement of the quantum geometric tensor and of the anomalous Hall drift, Nature **578**, 381 (2020).

[68] R. Resta, The insulating state of matter: A geometrical theory, European Physical Journal B **79**, 121 (2011), arXiv:1012.5776.

[69] R. Resta, Drude weight and superconducting weight, Journal of Physics: Condensed Matter **30**, 414001 (2018).

[70] A. Marrazzo and R. Resta, Local Theory of the Insulating State, Physical Review Letters **122**, 166602 (2019), arXiv:1807.01063.

[71] G. Bellomia and R. Resta, Drude weight in systems with open boundary conditions, Physical Review B **102**, 205123 (2020), arXiv:2007.04143.

[72] T. S. Jackson, G. Möller, and R. Roy, Geometric stability of topological lattice phases, Nature Communications **6**, 1 (2015), arXiv:1408.0843.

[73] Y. Gao, S. A. Yang, and Q. Niu, Geometrical effects in orbital magnetic susceptibility, Physical Review B **91**, 214405 (2015).

[74] A. Raoux, F. Piéchon, J. N. Fuchs, and G. Montambaux, Orbital magnetism in coupled-bands models, Physical Review B - Condensed Matter and Materials Physics **91**, 10.1103/PhysRevB.91.085120 (2015), arXiv:1411.5940.

[75] F. Piéchon, A. Raoux, J.-N. Fuchs, and G. Montambaux, Geometric orbital susceptibility: Quantum metric without Berry curvature, Physical Review B **94**, 134423 (2016).

[76] J.-W. Rhim, K. Kim, and B.-J. Yang, Quantum distance and anomalous Landau levels of flat bands, Nature **584**, 59 (2020).

[77] A. Srivastava and A. Imamoğlu, Signatures of Bloch-Band Geometry on Excitons: Nonhydrogenic Spectra in Transition-Metal Dichalcogenides, Physical Review Letters **115**, 166802 (2015).

[78] T. B. Smith, L. Pullasseri, and A. Srivastava, Momentum-space Gravity from the Quantum Geometry and Entropy of Bloch Electrons, (2021), arXiv:2108.02216.

[79] N. Regnault and B. A. Bernevig, Fractional Chern Insulator, Physical Review X **1**, 021014 (2011).

[80] E. I. Blount, Bloch Electrons in a Magnetic Field, Physical Review **126**, 1636 (1962).

[81] J.-W. Rhim and B.-J. Yang, Classification of flat bands according to the band-crossing singularity of Bloch wave functions, Physical Review B **99**, 1 (2019).

[82] S. Peotta and P. Törmä, Superfluidity in topologically nontrivial flat bands, Nature Communications **6**, 8944 (2015), arXiv:1506.02815.

[83] A. Julku, S. Peotta, T. I. Vanhala, D.-H. Kim, and P. Törmä, Geometric Origin of Superfluidity in the Lieb-Lattice Flat Band, Physical Review Letters **117**, 045303 (2016).

[84] L. Liang, T. I. Vanhala, S. Peotta, T. Siro, A. Harju, and P. Törmä, Band geometry , Berry curvature , and superfluid weight, Phys. Rev. B **95**, 024515 (2017), arXiv:1610.01803.

[85] L. Liang, S. Peotta, A. Harju, and P. Törmä, Wave-packet dynamics of Bogoliubov quasiparticles: Quantum metric effects, Physical Review B **96**, 1 (2017), arXiv:1705.04542.

[86] V. L. Berezinskiĭ, Destruction of Long-range Order in One-dimensional and Two-dimensional Systems having a Continuous Symmetry Group I. Classical Systems, Soviet Journal of Experimental and Theoretical Physics **32**, 493 (1971).

[87] J. M. Kosterlitz and D. J. Thouless, Ordering, metastability and phase transitions in two-dimensional systems, Journal of Physics C: Solid State Physics **6**, 1181 (1973).

[88] E. Y. Andrei and A. H. MacDonald, Graphene bilayers with a twist, Nature Materials **19**, 1265 (2020).

[89] E. Y. Andrei, D. K. Efetov, P. Jarillo-Herrero, A. H. MacDonald, K. F. Mak, T. Senthil, E. Tutuc, A. Yazdani, and A. F. Young, The marvels of moiré materials, Nature Reviews Materials **6**, 201 (2021).

[90] J.-X. Lin, Y.-H. Zhang, E. Morissette, Z. Wang, S. Liu, D. Rhodes, K. Watanabe, T. Taniguchi, J. Hone, and J. I. A. Li, Spin-orbit driven ferromagnetism at half moiré filling in magic-angle twisted bilayer graphene (2021), arXiv:2102.06566.

[91] D. J. Scalapino, S. R. White, and S.-C. Zhang, Superfluid density and the Drude weight of the Hubbard model, Physical Review Letters **68**, 2830 (1992).

[92] D. J. Scalapino, S. R. White, and S.-C. Zhang, Insulator, metal, or superconductor: The criteria, Physical Review B **47**, 7995 (1993).

[93] M. Xie and A. H. Macdonald, Nature of the Correlated Insulator States in Twisted Bilayer Graphene, Physical Review Letters **124**, 97601 (2020), arXiv:1812.04213.

[94] M. Serlin, C. L. Tschirhart, H. Polshyn, Y. Zhang, J. Zhu, K. Watanabe, T. Taniguchi, L. Balents, and A. F. Young, Intrinsic quantized anomalous Hall effect in a moiré heterostructure, Science **367**, 900 (2020), arXiv:1907.00261.

[95] S. Wu, Z. Zhang, K. Watanabe, T. Taniguchi, and E. Y. Andrei, Chern insulators, van Hove singularities and topological flat bands in magic-angle twisted bilayer graphene, Nature Materials **20**, 488 (2021).

[96] F. Xie, Z. Song, B. Lian, and B. A. Bernevig, Topology-Bounded Superfluid Weight in Twisted Bilayer Graphene, Physical Review Letters **124**, 167002 (2020), arXiv:1906.02213.

[97] Z. Song, Z. Wang, W. Shi, G. Li, C. Fang, and B. A. Bernevig, All Magic Angles in Twisted Bilayer Graphene are Topological, Physical Review Letters **123**, 36401 (2019).

[98] J. Ahn, S. Park, and B. J. Yang, Failure of Nielsen-Ninomiya Theorem and Fragile Topology in Two-Dimensional Systems with Space-Time Inversion Symmetry: Application to Twisted Bilayer Graphene at Magic Angle, Physical Review X **9**, 21013 (2019), arXiv:1808.05375.

[99] I. Kapon, Z. Salman, I. Mangel, T. Prokscha, N. Gavish, and A. Keren, a magnetic- fi eld-free stiffness meter viewpoint, Nature Communications **10**, 2463 (2019).

[100] S. Das Sarma, S. Adam, E. H. Hwang, and E. Rossi, Electronic transport in two dimensional graphene, Rev. Mod. Phys. **83**,

[101] X. Hu, T. Hyart, D. I. Pikulin, and E. Rossi, Geometric and conventional contribution to superfluid weight in twisted bilayer graphene, Physical Review Letters **123**, 237002 (2019), arXiv:1906.07152.

[102] F. Wu, A. H. MacDonald, and I. Martin, Theory of Phonon-Mediated Superconductivity in Twisted Bilayer Graphene, Physical Review Letters **121**, 257001 (2018), arXiv:1805.08735.

[103] Y. Alavirad and J. Sau, Ferromagnetism and its stability from the one-magnon spectrum in twisted bilayer graphene, Physical Review B **102**, 10.1103/PhysRevB.102.235123 (2020).

[104] F. Wu and S. Das Sarma, Quantum geometry and stability of moiré flatband ferromagnetism, Physical Review B **102**, 10.1103/PhysRevB.102.165118 (2020).

[105] B. A. Bernevig, B. Lian, A. Cowsik, F. Xie, N. Regnault, and Z.-D. Song, TBG V: Exact Analytic Many-Body Excitations In Twisted Bilayer Graphene Coulomb Hamiltonians: Charge Gap, Goldstone Modes and Absence of Cooper Pairing, arXiv:2009.14200 (2020).

[106] X. Hu, T. Hyart, D. I. Pikulin, and E. Rossi, Quantum-metric-enabled exciton condensate in double twisted bilayer graphene, arXiv:2008.03241 (2020), arXiv:2008.03241.

[107] L. V. Keldysh and Y. V. Kopaev, Possible instability of semimetallic state toward coulomb interaction, Soviet Phys. Solid State,ussr **6**, 2219 (1965).

[108] B. Halperin and T. Rice, The excitonic state at the semiconductor-semimetal transition (Academic Press, 1968) pp. 115 – 192.

[109] Y. E. Lozovik and V. I. Yudson, Feasibility of superfluidity of paired spatially separated electrons and holes - new superconductivity mechanism, Jetp Lett. **22**, 274 (1975).

[110] Y. E. Lozovik and V. I. Yudson, Novel mechanism of superconductivity - pairing of spatially separated electrons and holes, Zhurnal Eksperimentalnoi I Teoreticheskoi Fiziki **71**, 738 (1976).

[111] J. P. Eisenstein and A. H. MacDonald, Bose-einstein condensation of excitons in bilayer electron systems, Nature **432**, 691 (2004).

[112] M. M. Fogler, L. V. Butov, and K. S. Novoselov, High-temperature superfluidity with indirect excitons in van der Waals heterostructures, Nature Communications **5**, 4555 (2014).

[113] S. Gupta, A. Kutana, and B. I. Yakobson, Heterobilayers of 2D materials as a platform for excitonic superfluidity, Nature Communications **11**, 2989 (2020).

[114] Z. Wang, D. A. Rhodes, K. Watanabe, T. Taniguchi, J. C. Hone, J. Shan, and K. F. Mak, Evidence of high-temperature exciton condensation in two-dimensional atomic double layers, Nature **574**, 76 (2019).

[115] J. Wang, Q. Shi, E.-M. Shih, L. Zhou, W. Wu, Y. Bai, D. Rhodes, K. Barmak, J. Hone, C. R. Dean, and X.-Y. Zhu, Diffusivity reveals three distinct phases of interlayer excitons in $MoSe_2$/WSe_2 heterobilayers, Phys. Rev. Lett. **126**, 106804 (2021).

[116] T. Hazra, N. Verma, and M. Randeria, Bounds on the Superconducting Transition Temperature : Applications to Twisted Bilayer Graphene and Cold Atoms, Physical Review X **9**, 31049 (2019).

[117] A. Julku, T. J. Peltonen, L. Liang, T. T. Heikkilä, and P. Törmä, Superfluid weight and Berezinskii-Kosterlitz-Thouless transition temperature of twisted bilayer graphene, Physical Review B **101**, 060505 (2020), arXiv:1906.06313.

[118] F. Wu and S. Das Sarma, Quantum geometry and stability of moiré flatband ferromagnetism, Physical Review B **102**, 1 (2020), arXiv:2005.10254.

[119] J. M. Park, Y. Cao, K. Watanabe, T. Taniguchi, and P. Jarillo-Herrero, Tunable strongly coupled superconductivity in magic-angle twisted trilayer graphene, Nature **590**, 249 (2021).

[120] D. S. L. Abergel, M. Rodriguez-Vega, E. Rossi, and S. Das Sarma, Interlayer excitonic superfluidity in graphene, Phys. Rev. B **88**, 235402 (2013).

[121] J. Zhang and E. Rossi, Chiral superfluid states in hybrid graphene heterostructures, Phys. Rev. Lett. **111**, 086804 (2013).

[122] J. Zhang, C. Triola, and E. Rossi, Proximity effect in graphene˘topological-insulator heterostructures, Phys. Rev. Lett. **112**, 096802 (2014).

[123] C. Triola, D. M. Badiane, A. V. Balatsky, and E. Rossi, General Conditions for Proximity-Induced Odd-Frequency Superconductivity in Two-Dimensional Electronic Systems, Phys. Rev. Lett. **116**, 257001 (2016).

[124] K. Liu, L. Zhang, T. Cao, C. Jin, D. Qiu, Q. Zhou, A. Zettl, P. Yang, S. G. Louie, and F. Wang, Evolution of Interlayer Coupling in Twisted MoS2 Bilayers, ArXiv e-prints (2014), arXiv:1406.6487.

[125] F. Wu, T. Lovorn, E. Tutuc, I. Martin, and A. H. Macdonald, Topological Insulators in Twisted Transition Metal Dichalcogenide Homobilayers, Physical Review Letters **122**, 086402 (2019).

[126] M. Rodriguez-Vega, G. Schwiete, and E. Rossi, Spin-charge coupled transport in van der Waals systems with random tunneling, Physical Review Research **1**, 033085 (2019), arXiv:arXiv:1904.01015v1.

[127] Y. S. Gani, H. Steinberg, and E. Rossi, Superconductivity in twisted graphene NbSe2 heterostructures, Physical Review B **99**, 235404 (2019), arXiv:1903.00475.

[128] E. C. Regan, D. Wang, C. Jin, M. I. Bakti Utama, B. Gao, X. Wei, S. Zhao, W. Zhao, Z. Zhang, K. Yumigeta, M. Blei, J. Carlstrøm, K. Watanabe, T. Taniguchi, S. Tongay, M. Crommie, A. Zettl, and F. Wang, Mott and generalized Wigner crystal states in WSe2/WS2 moiré superlattices, Nature **579**, 359 (2020).

[129] Z. Zhang, Y. Wang, K. Watanabe, T. Taniguchi, K. Ueno, E. Tutuc, and B. J. LeRoy, Flat bands in twisted bilayer transition metal dichalcogenides, Nature Physics **16**, 1093 (2020).

[130] Y. Xu, S. Liu, D. A. Rhodes, K. Watanabe, T. Taniguchi, J. Hone, V. Elser, K. F. Mak, and J. Shan, Correlated insulating states at fractional fillings of moiré superlattices, Nature **587**, 214 (2020).

[131] E. Rossi and C. Triola, Van Der Waals Heterostructures with Spin-Orbit Coupling, Annalen der Physik **532**, 1900344 (2020), arXiv:1909.11674.

[132] A. Ghiotto, E.-M. Shih, G. S. S. G. Pereira, D. A. Rhodes, B. Kim, J. Zang, A. J. Millis, K. Watanabe, T. Taniguchi, J. C. Hone, L. Wang, C. R. Dean, and A. N. Pasupathy, Quantum criticality in twisted transition metal dichalcogenides (2021), arXiv:2103.09796 [cond-mat.mes-hall].

[133] C.-P. Lu, M. Rodriguez-Vega, G. Li, A. Luican-Mayer, K. Watanabe, T. Taniguchi, E. Rossi, and E. Y. Andrei, Local, global, and nonlinear screening in twisted double-layer graphene, Proceedings of the National Academy of Sciences **113**, 6623 (2016).

[134] X.-L. Qi, T. L. Hughes, and S.-C. Zhang, Chiral topological superconductor from the quantum Hall state, Physical Review B **82**, 184516 (2010), arXiv:1003.5448.